Biosensors and Bioelectronics 26 (2011) 3240–3245

Contents lists available at ScienceDirect

Biosensors and Bioelectronics

journal homepage: www.elsevier.com/locate/bios

35 MHz quartz crystal microbalance and surface plasmon resonance studies on the binding of angiotensin converting enzyme with lisinopril

Zhaohong Su, Li Chen, Ying Liu, Xiuhui He, Yaping Zhou, Qingji Xie*, Shouzhuo Yao

Key Laboratory of Chemical Biology and Traditional Chinese Medicine Research (Ministry of Education of China), College of Chemistry and Chemical Engineering, Hunan Normal University, Changsha 410081, PR China

ARTICLE INFO

Article history:
Received 17 September 2010
Received in revised form
12 December 2010
Accepted 21 December 2010
Available online 28 December 2010

Keywords:
Angiotensin converting enzyme
Lisinopril
Interaction parameters
35-MHz quartz crystal microbalance
Surface plasmon resonance

ABSTRACT

Angiotensin converting enzyme (ACE) plays a pivotal role in blood pressure regulation, and its interaction with an ACE inhibitor (ACEI) is an important research topic for treatment of hypertension. Herein, a low reagent consumption, multiparameter and highly sensitive quartz crystal microbalance (QCM) at 35-MHz fundamental frequency was utilized to monitor *in situ* the binding process of solution lisinopril (LIS, a carboxylic third-generation ACEI) to ACE adsorbed at a 1-dodecanethiol (C12SH)-modified Au electrode. From the QCM data, the binding molar ratio (r) of LIS to adsorbed ACE was estimated to be 2.3:1, and the binding and dissociation rate constants (k_1 and k_{-1}) and the binding equilibrium constant (K_a) were estimated to be $k_1 = 4.1 \times 10^6\ L\,mol^{-1}\,s^{-1}$, $k_{-1} = 7.3 \times 10^{-3}\ s^{-1}$ and $K_a = 5.62 \times 10^8\ L\,mol^{-1}$, respectively. Comparable qualitative and quantitative results were also obtained from separate experiments of cyclic voltammetry, electrochemical impedance spectroscopy and surface plasmon resonance measurements.

1. Introduction

Some enzymes are important drug targets for developing new drugs against various diseases, e.g. cancers, AIDS, diabetes and hypertension (Cushman and Ondetti, 1999; Johnson et al., 2002; Noble et al., 2004). Angiotensin converting enzyme (ACE; peptidyl dipeptide hydrolase, EC 3.4.15.1) is a membrane-bound glycoprotein localized in endothelial, epithelial, neuroepithelial and male germinal cells (Bernstein et al., 1989; Hubert et al., 1991; Kumar et al., 1991; Ryan et al., 1975; Soubrier et al., 1988). ACE is a Zn^{2+}-containing metalloprotease that can catalyze the conversion of the inactive decapeptide angiotensin I to the potent vasoconstricting octapeptide angiotensin II and thus abrogate the vasodilator function of bradykinin (Jimsheena and Gowda, 2009; Skeggs et al., 1954). Hence, ACE plays a pivotal role in the homeostatic mechanism of mammals for regulation of blood pressure and fluid balance (Erdös, 1976; Jimsheena and Gowda, 2009; Peach, 1977). Some synthetic ACE inhibitors (ACEI) are effective in the treatment of hypertension and congestive heart failure (Brown and Vaughan, 1998; Mancini et al., 1996). Lisinopril (LIS) is a carboxylic third-generation ACEI developed after captopril and enalapril for hypertension treatment (Bussien et al., 1985), the binding of which to ACE results mainly from electrostatic interactions, hydrogen bonds and aromatic stacking (Ehlers and Riordan, 1991; Fernandez et al., 2003), as schematically depicted in Scheme 1.

Thus far, many methods have been proposed to study the interactions of ACE with active molecules (ACEI) for developing drugs against hypertension and heart failure, and it is an important theme to identify the inhibitors for a given enzyme target from a library of compounds (Oliver von and Bömer, 2005). Ultraviolet–visible spectrophotometry (Chang et al., 2001; Matsui et al., 1992), fluorescence-based techniques (Sentandreu and Toldra, 2006), high-performance liquid chromatography (Wu et al., 2002) and capillary electrophoresis (Tang and Kang, 2006; Zhang et al., 2000) were used to investigate ACEI screening based on solution or immobilized ACE. However, the real-time information on the kinetics of ACEI–ACE binding is still rather limited and the consumption of expensive ACE is usually high. Therefore, developing a rapid, low-cost, and effective technique to study ACEI–ACE binding is interesting and important.

The quartz crystal microbalance (QCM) is a powerful quantitative tool to investigate various modified substances on an electrode and monitor *in situ* the electrode-modification processes (Buttry and Ward, 1992; Xie et al., 1999a). The QCM, with a piezoelectric quartz crystal (PQC) as its central sensing element, can dynamically detect a change in mass loading on the electrode surface down to the monolayer or submonolayer level, the viscoelasticity of a film modified on the electrode, and the solution viscosity/density near

* Corresponding author. Tel.: +86 731 88865515; fax: +86 731 88865515.
E-mail address: xieqj@hunnu.edu.cn (Q. Xie).

0956-5663/$ – see front matter © 2010 Elsevier B.V. All rights reserved.
doi:10.1016/j.bios.2010.12.033

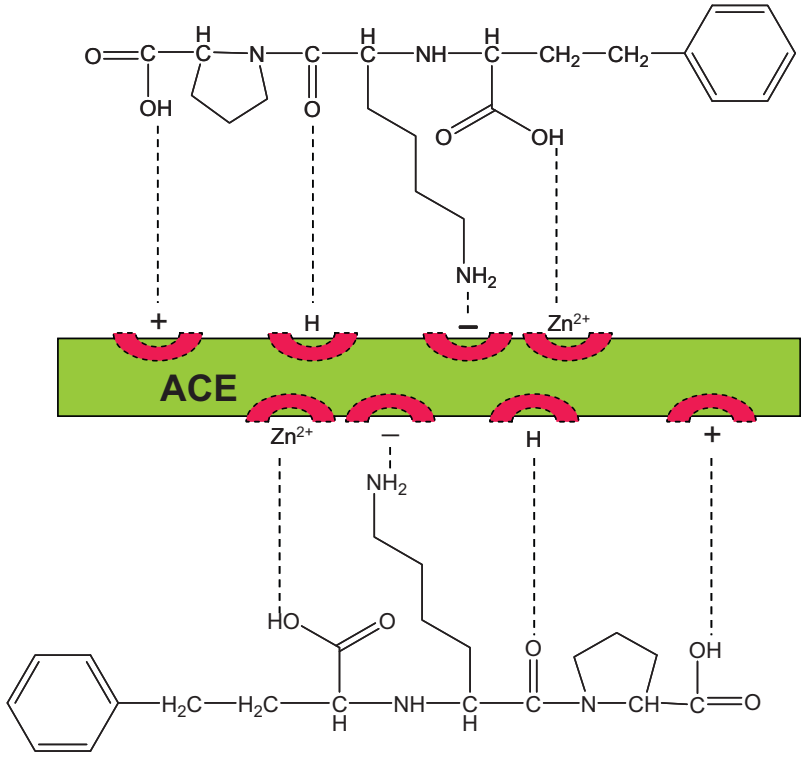

Scheme 1. A simplified mechanism probably responsible for the binding of ACE with LIS.

the QCM electrode. The mass effect of the QCM frequency can be depicted by the Sauerbrey equation, and its net viscosity/density effect can be quantified on the basis of the equations proposed by Kanazawa and Martin et al. (Martin et al., 1991; Noel and Topart, 1994; Xie et al., 1999a). The impedance-analysis-based QCM can provide multidimensional piezoelectric information on the resonant frequency (f_0), motional resistance (R_1), and etc., which has been successfully used to study the binding of small molecules with biomacromolecules (9-MHz QCM) (He et al., 2005; Liu et al., 2006; Zhang et al., 2005). Conventional QCM biosensors use 5–10 MHz crystals with limited sensitivity. Recently, in order to enhance the sensitivity of QCM biosensors, QCMs at 15-MHz (Albyn, 2001), 27-MHz (Furusawa et al., 2009; Nishino et al., 2004; Takahashi et al., 2009), 50-MHz (Lederera et al., 2010), 62-MHz (Kao et al., 2008), 96-MHz (Williams et al., 2007) and higher fundamental frequencies (Ogi et al., 2009) were reported. QCMs at fundamental frequencies higher than ca. 40 MHz have very thin crystal wafer and need special fabrication and engineering, which are thus limited for wide applications in conventional laboratories due to their commercial unavailability. As we are aware, the impedance-analysis-based and commercially available 35-MHz QCM has not been reported for monitoring of drug target-drug interactions, which provides an enhanced sensitivity for such process studies, as discussed in Supplementary information.

Herein, we use a low reagent consumption, multiparameter and highly sensitive 35-MHz QCM to monitor *in situ* the binding process of solution LIS to ACE adsorbed at a 1-dodecanethiol (C12SH)-modified Au electrode, and the binding and dissociation rate constants (k_1 and k_{-1}), the binding equilibrium constant (K_a), and the binding molar ratio (r) are estimated. Since the adsorption amount of ACE here is in the sub-microgram scale, our method requires a very low consumption of the expensive drug target in each run. The QCM results are quantitatively supported by surface plasmon resonance (SPR) experiments.

2. Experimental

2.1. Instrumentation and chemicals

A computer-interfaced HP4395A impedance analyzer was employed. AT-cut 35-MHz PQCs with 6-mm wafer diameter (Beijing Chenjing Electronics Co., LTD, China) were used. The Au electrode with 2.0-mm diameter (keyhole configuration, area = $0.03 \pm 0.002\ cm^2$) on one side of the PQC was exposed to the solution and served as the working electrode, while that on the other side faced air. The random frequency noise of the 35-MHz QCM was ca. ±5 Hz in buffer solution, and the frequency drifting was within ±2 Hz for 30 min. The fast Fourier transform analysis was applied to smooth the raw data to reduce random noises, which did not affect the kinetic parameters (Furusawa et al., 2009). AT-cut 9-MHz PQCs with 12.5-mm wafer diameter and 6-mm electrode diameter (Model JA5, Beijing Chenjing Electronics Co., Ltd., China) were used for comparison. All electrochemical experiments were conducted on a CHI660C electrochemical workstation (CH Instrument Co., USA). The reference electrode was a KCl-saturated calomel electrode (SCE), and a carbon rod served as the counter electrode. All potentials reported here are cited versus SCE. An Autolab SPR (Eco Chemie, The Netherlands) was employed for comparative measurements.

ACE, LIS and C12SH were purchased from Sigma and used as received. The experiments were conducted in 50 mmol L^{-1} phosphate buffer solution (PBS, 2.5 mmol L^{-1} NaH_2PO_4 + 47.5 mmol L^{-1} Na_2HPO_4 + 300 mmol L^{-1} NaCl, pH 8.0). The sample solutions were prepared with the PBS and stored at 4 °C when not in use. All chemicals were analytical grade or better. Milli-Q ultrapure water (>18 MΩ cm) and fresh prepared solutions were used throughout the experiments. All experiments were carried out at room temperature around 20 °C.

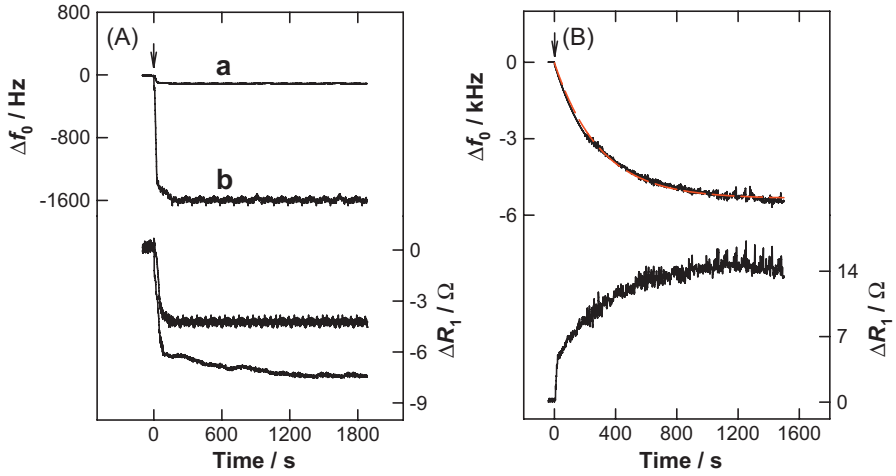

Fig. 1. (A) QCM responses during adsorption of 10 mmol L^{-1} C12SH onto bare 9-MHz (a) and 35-MHz (b) QCM Au electrodes in absolute ethanol. The arrow indicates the moment of addition of C12SH in the detection cell. (B) 35-MHz QCM responses at C12SH/Au to the addition of 2.15 μmol L^{-1} ACE into PBS. The arrow indicates the moment of ACE addition. The red curve shows the fitted results according to Eq. (1). (For interpretation of the references to color in this figure legend, the reader is referred to the web version of the article.)

2.2. Procedures

At first, the QCM Au electrode was carefully cleaned by pipetting one drop of fresh Piranha solution (H_2SO_4:H_2O_2, v/v 3:1) on its surface and kept for 3 min, then rinsing it with copious Milli-Q ultrapure water. The treatment was repeated three times. The treated electrode was then scanned between 0 and 1.5 V vs. SCE in 0.2 mol L^{-1} $HClO_4$ at 50 mV s^{-1} for sufficient number of cycles to obtain reproducible cyclic voltammograms.

The thus-treated QCM Au electrode was placed in absolute ethanol under magnetic stirring, and 10 mmol L^{-1} C12SH (final concentration) was added after the QCM baseline responses became stable. The C12SH/Au electrode was obtained after equilibrium adsorption of C12SH on Au.

The C12SH/Au electrode was located in a specially designed 50 μL detection cell containing PBS under magnetic knocking of the tube supporting the PQC, and 0.28 μg μL^{-1} ACE (final concentration, saturated for adsorption) was added after the QCM baseline responses became stable. The ACE/C12SH/Au electrode was obtained after equilibrium adsorption of ACE.

The ACE/C12SH/Au electrode was placed in PBS. After the QCM baseline responses became stable, a given volume of stock solution of LIS (50 μmol L^{-1}) was added into the stirred buffer solution. The QCM parameters on the LIS–ACE interaction were recorded. The QCM Au electrodes modified with C12SH, ACE/C12SH and LIS/ACE/C12SH were characterized by cyclic voltammetry (CV) and electrochemical impedance spectroscopy (EIS) in PBS containing 2 mmol L^{-1} $K_4Fe(CN)_6$. The 35-MHz QCM experiments using three different 35-MHz crystals gave well reproducible frequency responses for adsorption of C12SH and ACE, and then binding of LIS, and the RSD of K_a obtained from the three crystals was within ±7%.

Commercially available Au thin-film electrodes with an Au-film thickness of 50 nm were used as the working electrode for SPR measurements in a specially designed cell. The apparent surface area exposing to the solution was 3.14 mm^2. Solutions were added to the electrolytic cell using a sample injector, and then were pumped out (Jiang et al., 2008). Before and after each measurement, the cell and the electrodes were rinsed with Milli-Q ultrapure water three times. The successive experimental operations of C12SH adsorption, ACE adsorption and LIS–ACE binding at the SPR Au electrode were similar to those at the QCM Au electrode as above.

3. Results and discussion

3.1. QCM studies

As we are aware, the thiol pretreatment of the gold electrodes may prevent possible conformational change resulting from the bonding of the sulfide moieties of protein to the gold surface (Xie et al., 1999b). In addition, protein adsorption is very strong and more significant on a hydrophobic surface through hydrophobic interaction (Prime and Whitesides, 1991). Here, the Au electrode was pretreated by C12SH before ACE adsorption. Fig. 1A shows the 35-MHz QCM responses during adsorption of C12SH onto bare Au electrode in absolute ethanol. After quick injection of 10 mmol L^{-1} C12SH (final concentration) into absolute ethanol, the frequency and resistance decreased simultaneously, and final frequency and resistance decreases by ca. −1600 Hz and −7.5 Ω were obtained, respectively. The $|\Delta f_0/\Delta R_1|$ ratio of 213 Hz Ω^{-1} here is larger than that for a net viscodensity effect ($|\Delta f_{0L}/\Delta R_{1L}|$ = 65 Hz Ω^{-1} for 35-MHz QCM, see Supplementary information for details), demonstrating the high rigidity of the adsorbed C12SH film. When another aliquot of C12SH solution was added later, negligible frequency and resistance changes were found (not plotted), implying that an almost full self-assembly had already formed. For comparison, adsorption of C12SH on a 9-MHz QCM electrode was conducted, and a final frequency decrease only by ca. −120 Hz was found (Fig. 1A), validating the higher sensitivity of the 35-MHz QCM as expected. The sensitivity-enhancement factor of 1600/120 = 13.3 obtained experimentally is slightly smaller than the theoretical value of $(35/9)^2$ = 15.1 derived from the Sauerbrey equation, resulting probably from the different surface-roughness factors of the 35-MHz and 9-MHz PQCs. Our CV and EIS experiments suggest that the C12SH molecules adsorbed at Au notably blocked the electronic communication between solution-state $[Fe(CN)_6]^{3-/4-}$ and the Au electrode, as shown in Fig. 2, and such electroactivity-blocked effects induced by thiol adsorption are well known (Bard and Faulkner, 2001).

Fig. 1B shows the typical adsorption curves of ACE at C12SH/Au. The ACE addition resulted in a quick f_0 decrease and a quick R_1 increase, then both parameters leveled off after ca. 1200 s, indicating the arrival of adsorption equilibrium. The final $|\Delta f_0/\Delta R_1|$ ratio for ACE adsorption is estimated to be 389 Hz Ω^{-1}, also indicating that the mass loading took a dominant effect on the total frequency shift. The adsorption of ACE onto C12SH/Au obeys first-order kinet-

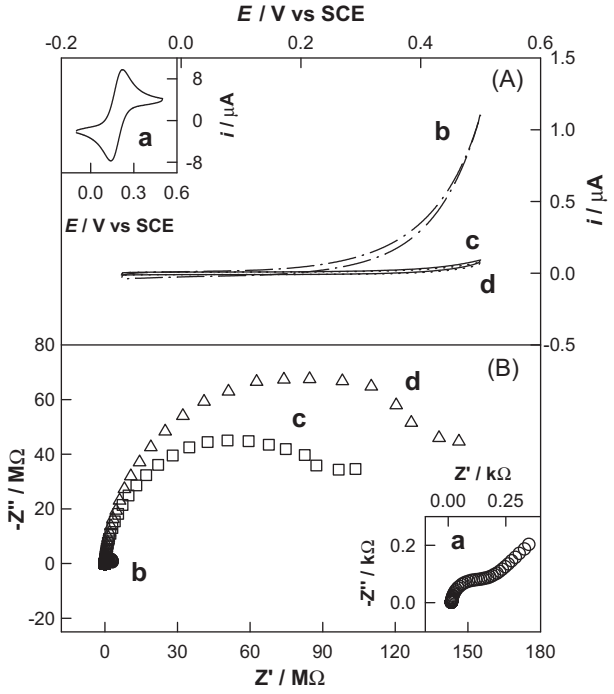

Fig. 2. Cyclic voltammograms (A) and EIS (B) at bare (a), C12SH- (b), ACE/C12SH- (c) and LIS/ACE/C12SH-modified (d) Au electrodes in PBS containing 2 mmol L^{-1} $K_4Fe(CN)_6$. Scan rate: 50 mV s^{-1}. EIS parameters: 100 kHz to 0.001 Hz, 10 mV rms, 0.18 V vs. SCE.

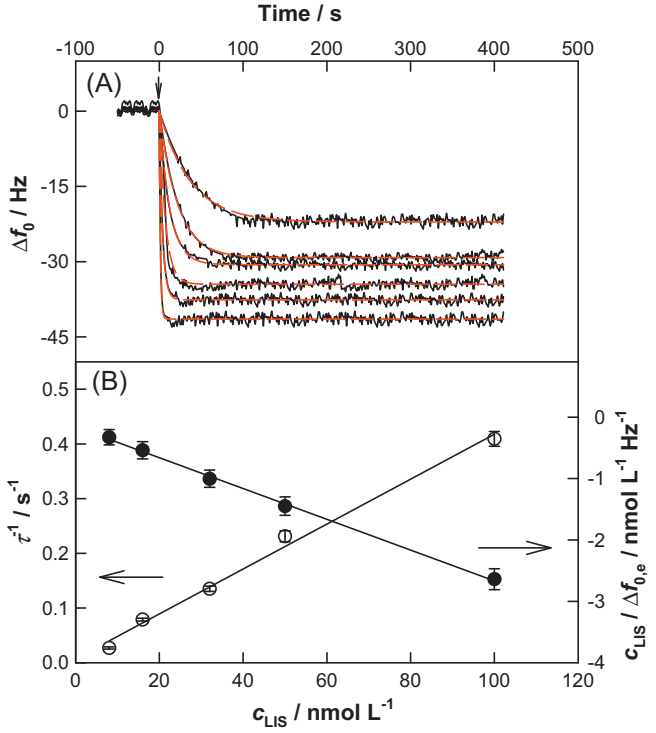

Fig. 3. Frequency responses at ACE/C12SH/Au to additions of LIS at different concentrations (8.00, 16.0, 32.0, 50.0, 100, and 400 nmol L^{-1}) into PBS (A), and $c_{LIS}/\Delta f_{0,e}$ and τ^{-1} as functions of c_{LIS} (B). The arrow indicates the moment of LIS addition. The red curves show the fitted results according to Eq. (9).

ics with the following equation (Mao et al., 2002):

$$\Delta f_0 = \Delta f_{0,\max}(1 - e^{-k_1 c_0 t}) \quad (1)$$

where k_1 is the rate constant of the forward reaction (adsorption), and c_0 is the initial concentration of ACE in solution. Fitting the time-dependent Δf_0 response for ACE adsorption shown in Fig. 1B to Eq. (1) via the SigmaPlot V2.0 software returns $\Delta f_{0,\max} = -5353$ Hz (corresponding to 0.015 nmol cm^{-2} of ACE) and $k_1 = 1570$ L mol^{-1} s^{-1}, respectively.

Fig. 3A shows the 35-MHz QCM responses to binding of solution-state LIS at different concentrations with ACE adsorbed on C12SH/Au. The additions of LIS immediately decreased f_0, and all the $|\Delta f_0/\Delta R_1|$ values were larger than 65 Hz Ω^{-1}, suggesting that the mass effect also dominated the frequency change and the Sauerbrey equation is reasonably valid for estimations of interaction parameters. Control experiments suggested that no obvious frequency changes were observed in similar experiments either using a ACE-free C12SH/Au electrode or after addition of the PBS blank solution (not plotted).

CV (Fig. 2A) and EIS (Fig. 2B) experiments were conducted in PBS containing 2 mmol L^{-1} $K_4Fe(CN)_6$ after ACE immobilization and LIS–ACE binding. It is clear that the redox couple of $[Fe(CN)_6]^{3-}/[Fe(CN)_6]^{4-}$ exhibited a more irreversible behavior after the ACE immobilization and further LIS–ACE binding, suggesting that the electrode surface was occupied by insulating species to a more significant extent and the electron exchange ability on the electrode become weaker, which validates the occurrence of ACE immobilization and LIS–ACE binding.

The LIS–ACE binding on the electrode surface can be described by the following equation:

$$[\text{free binding site}]_s + [\text{LIS}]_l \rightleftharpoons [\text{LIS-bound site}]_s \quad (2)$$

where the subscripts of "s" and "l" denote "on electrode surface" and "in liquid solution", respectively.

When the reaction reaches equilibrium, K_a can be expressed as

$$K_a = \frac{c_{B,LIS}}{c_s c_{F,LIS}} \quad (3)$$

where $c_{B,LIS}$ and c_s denote the equilibrium surface concentrations of bound LIS and free site per surface area, respectively, and $c_{F,LIS}$ is the equilibrium concentration of free LIS in solution. By simplifying the Sauerbrey equation to $\Delta f_0 = -k\Delta m$, where Δm is in g cm^{-2}, $c_{B,LIS}$ and c_s can be expressed as

$$c_{B,LIS} = -\frac{\Delta f_{0,e}}{kM_{LIS}} \quad (4)$$

$$c_s = -\frac{\Delta f_{0,\max} - \Delta f_{0,e}}{kM_{LIS}} \quad (5)$$

where $\Delta f_{0,e}$ is the frequency shift after equilibrium at a specified LIS concentration, and $\Delta f_{0,\max}$ is the maximum frequency shift when all of the binding sites are occupied.

Considering a negligible change in the concentration of solution LIS after its binding to adsorbed ACE, one obtains the following equation (Ebara and Okahata, 1994; Liu et al., 2006; Uzawa et al., 2002):

$$\frac{c_{LIS}}{\Delta f_{0,e}} = \frac{c_{LIS}}{\Delta f_{0,\max}} + \frac{1}{K_a \Delta f_{0,\max}} \quad (6)$$

As shown in Fig. 3B, $c_{LIS}/\Delta f_{0,e}$ is well linear with LIS concentration from 8 to 100 nmol L^{-1}, with a regression equation of $c_{LIS}/\Delta f_{0,e}$ (nmol L^{-1} Hz^{-1}) = $-0.0256 c_{LIS}$ (nmol L^{-1}) $- 0.015$ and a linearity correlation coefficient of 0.998. Therefore, the K_a value is calculated to be 1.71×10^9 L mol^{-1}, which agrees well with those reported based on a displacement isothermal titration calorimetry method (Montserrat et al., 2007) (2.6×10^9 L mol^{-1}), and equilibrium dialysis (Wei et al., 1992) (4.2×10^9 L mol^{-1}), implying that the results obtained from the 35-MHz QCM is reliable.

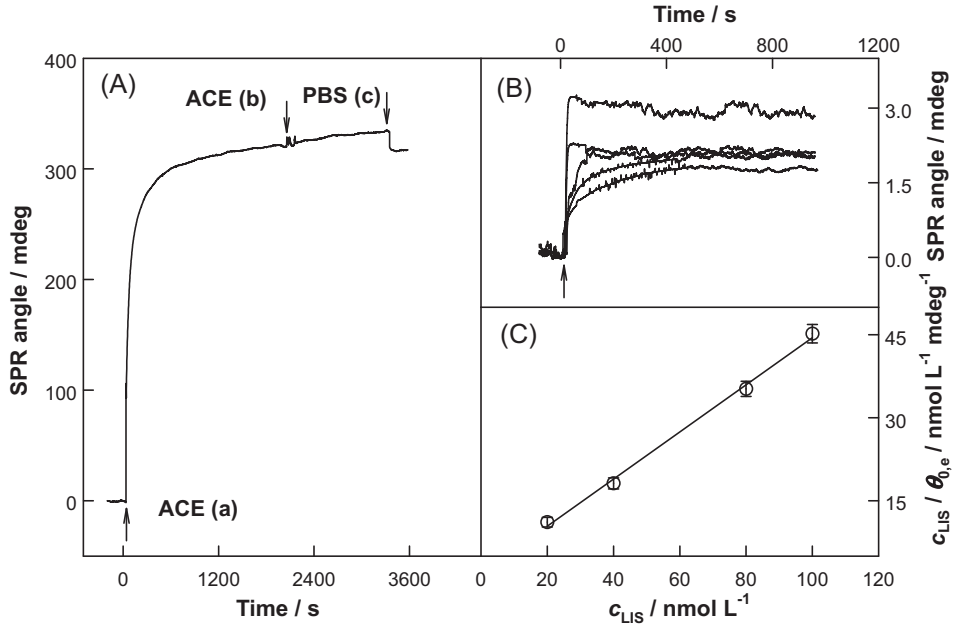

Fig. 4. (A) Real-time SPR responses at C12SH/Au. The arrows indicate additions of 2.15 μmol L^{-1} ACE into PBS (a and b) and rinse with PBS (c). (B) Real-time SPR responses at ACE/C12SH/Au to additions of LIS at different concentrations (20.0, 40.0, 80.0, 100, and 400 nmol L^{-1}) into PBS and (C) $c_{LIS}/\theta_{0,e}$ as a function of c_{LIS}. The arrow indicates the moment of LIS addition.

In addition, the binding molar ratio (r) of LIS to ACE can be calculated below from the frequency response and the Sauerbrey equation (Sauerbrey, 1959),

$$\frac{n_{LIS}}{n_{ACE}} = \left(\frac{W_{LIS}}{M_{LIS}}\right) : \left(\frac{W_{ACE}}{M_{ACE}}\right) \quad (7)$$

$$n_{LIS} : n_{ACE} = \frac{M_{ACE} \times \Delta f_{0,LIS}}{M_{LIS} \times \Delta f_{0,ACE}} \quad (8)$$

where n_{LIS} and n_{ACE} are the amounts of LIS and ACE in mol, W_{LIS} and W_{ACE} are the mass of LIS and ACE on the electrode surface in g, M_{LIS} and M_{ACE} are the molar mass of LIS (405.5) and ACE (130,000) (Mayer and Meyer, 2000), respectively, and $\Delta f_{0,ACE}$ (−5353 Hz here) and $\Delta f_{0,LIS}$ (−39 Hz here) are the frequency shifts caused by the equilibrium adsorption of ACE and the saturated LIS interaction with ACE, respectively. The molar ratio of LIS to the immobilized ACE calculated from Eq. (8) is 2.3:1, which agrees well with the value of 2:1 reported based on active site titration (Ehlers and Riordan, 1991).

The kinetics constants of LIS binding to ACE can also be calculated from the dynamic frequency vs. time responses shown in Fig. 3A. The binding amount formed at time t after addition of LIS is given by Okahata et al. (Okahata et al., 1998)

$$\Delta f_0 = \Delta f_{0,max}(1 - e^{-(1/\tau)t}) \quad (9)$$

where Δf_0 and $\Delta f_{0,max}$ are the frequency changes at time t and $t \to \infty$, respectively.

Hence, $\Delta f_{0,max}$ and the reciprocal of the relaxation time (τ^{-1}) can be obtained through fitting experiment data in Fig. 3A, and the results are listed in Table 1S. The quality of the fitting can be evaluated with the relative sum of the residual square as $q_r = \sum_1^N (\Delta f_{0,fit} - \Delta f_{0,expt})^2 / \sum_1^N \Delta f_{0,expt}{}^2$, here $\Delta f_{0,fit}$ and $\Delta f_{0,expt}$ refer to the values of frequency shift obtained by way of fitting method and experiment, respectively, and N is the number of the response signal points. The small values of q_r in Table 1S indicate that the fitting here is good.

In addition, the following equation displays a relationship between the relaxation rate constant (τ^{-1}) and the initial LIS concentration $c_{0,LIS}$ (Mao et al., 2002),

$$\tau^{-1} = k_1 c_{0,LIS} + k_{-1} \quad (10)$$

If the binding processes at different LIS concentration were monitored, a series of τ^{-1} and $\Delta f_{0,max}$ can be obtained according to Eq. (9). Then, the kinetics parameters, k_1 and k_{-1}, can be determined from Eq. (10), and the binding equilibrium constant, K_a, can be thus obtained,

$$K_a = \frac{k_1}{k_{-1}} \quad (11)$$

Fig. 3B shows a linear correlation between the reciprocal of the relaxation time (τ^{-1}) of the binding and the concentration of LIS, with a correlation coefficient of 0.997. The values of k_1 and k_{-1} are estimated from the slope and intercept to be 4.1×10^6 L mol^{-1} s^{-1} and 7.3×10^{-3} s^{-1}, respectively. The binding equilibrium constant K_a is calculated to be 5.62×10^8 L mol^{-1}. The K_a value obtained from Eq. (11) is acceptably consistent with that obtained from Eq. (6).

3.2. SPR studies

In addition, the LIS–ACE interaction was examined by SPR technique. SPR is based on the reflection of an incident light on a surface when a fraction of the optical energy is absorbed by surface plasmon, and the response of the SPR resonant angle is very sensitive to the change in the property and the adsorbent state of the exterior medium at the solid/liquid interface (Janshoff et al., 2000; Jiang et al., 2008). Fig. 4A shows the SPR response at C12SH/Au to addition of 2.15 μmol L^{-1} ACE into PBS. The resonance angle increased as soon as the addition of ACE into the detection solution. When another aliquot of ACE solution was added after the 2000−s adsorption, a negligible SPR angle change was found, indicating saturated adsorption. After reacting for 3000 s and washed with PBS, the resonance angle shift resulting from the ACE−saturated adsorption is about 310 mdeg. Fig. 4B shows the binding responses of the

ACE–saturated electrode in PBS to additions of LIS at different concentrations. If assuming that the SPR angle shift (θ) after the binding is proportional to the bound LIS, the following equation similar to Eq. (6) is applicable (Wegner et al., 2004),

$$\frac{c_{LIS}}{\theta_{0,e}} = \frac{c_{LIS}}{\theta_{0,max}} + \frac{1}{K_a\theta_{0,max}} \quad (12)$$

where $\theta_{0,e}$ is the SPR angle shift after equilibrium at a specified LIS concentration, and $\theta_{0,max}$ is the maximum SPR angle shift when all of the binding sites are occupied. As shown in Fig. 4C, $c_{LIS}/\theta_{0,e}$ is well linear with LIS concentration from 20 to 100 nmol L^{-1}, with a regression equation of $c_{LIS}/\theta_{0,e}$ (nmol L^{-1} mdeg^{-1}) = 0.429c_{LIS} (nmol L^{-1}) + 0.181 and a linearity correlation coefficient of 0.997. Therefore, the K_a value is calculated to be 2.4×10^9 L mol^{-1}, which agrees well with the above QCM results.

In addition, the r value of solution LIS to adsorbed ACE can be approximately calculated according to the following equation:

$$n_{LIS} : n_{ACE} = \frac{M_{ACE} \times \theta_{0,LIS}}{M_{LIS} \times \theta_{0,ACE}} \quad (13)$$

where $\theta_{0,ACE}$ (310 mdeg in this case) and $\theta_{0,LIS}$ (2.3 mdeg in this case) are the SPR angle shifts caused by the adsorption of ACE and the LIS interaction with ACE in saturation, respectively. The molar ratio of LIS to the immobilization ACE calculated from Eq. (13) is 2.4:1, which agrees well with that obtained from the above 35-MHz QCM.

4. Conclusion

A commercially available, low reagent consumption, multiparameter and highly sensitive 35-MHz QCM has been proposed to monitor *in situ* the binding process of solution LIS to ACE adsorbed at a C12SH-modified Au electrode and acquire the interaction parameters. The impedance analysis mode of the 35-MHz QCM is convenient in experimental operations and can provide information on the film-rigidity validation when using the Sauerbrey equation to calculate the kinetics constants. The r and K_a values obtained from the independent 35-MHz QCM and SPR are well comparable, which also agree well with the values previously reported in the literatures (Ehlers and Riordan, 1991; Montserrat et al., 2007; Wei et al., 1992). To our knowledge, the 35 MHz QCM here uses the highest fundamental frequency of commercially available PQCs reported to date, and this work may have presented a novel and easily popularized experimental platform to study the interactions of many other biomolecules for biomedical and biosensor applications.

Acknowledgements

This work was supported by the National Natural Science Foundation of China (21075036, 90713018), the State Special Scientific Project on Water Treatment (2009ZX07212-001-06), and the Foundations of Hunan Provincial Education Department (05K009) and State Key Laboratory of Chemo/Biosensing and Chemometrics (200902).

Appendix A. Supplementary data

Supplementary data associated with this article can be found, in the online version, at doi:10.1016/j.bios.2010.12.033.

References

Albyn, K.C., 2001. J. Chem. Eng. Data 46, 1415–1416.
Bard, A.J., Faulkner, L.R., 2001. Electrochemical methods Fundamentals and Applications, second ed. Wiley, New York.
Bernstein, K.E., Martin, B.M., Edwards, A.S., Bernstein, E.A., 1989. J. Biol. Chem. 264, 11945–11951.
Brown, N.J., Vaughan, D.E., 1998. Circulation 97, 1411–1420.
Bussien, J.P., Waeber, B., Nussberger, J., Gomez, H.J., Brunner, H.R., 1985. Curr. Ther. Res. 37, 342–351.
Buttry, D.A., Ward, M.D., 1992. Chem. Rev. 92, 1355–1379.
Chang, B., Chen, R.L.C., Huang, I.J., Chang, H., 2001. Anal. Biochem. 291, 84–88.
Cushman, D.W., Ondetti, M.A., 1999. Nat. Med. 5, 1110–1112.
Ebara, Y., Okahata, Y., 1994. J. Am. Chem. Soc. 116, 11209–11212.
Ehlers, M.R.W., Riordan, J.F., 1991. Biochemistry 30, 7118–7126.
Erdös, E.G., 1976. Am. J. Med. 60, 749–759.
Fernandez, J.H., Hayashi, M.A.F., Camargo, A.C.M., Neshich, G., 2003. Biochem. Biophys. Res. Commun. 308, 219–226.
Furusawa, H., Komatsu, M., Okahata, Y., 2009. Anal. Chem. 81, 1841–1847.
He, H., Xie, Q., Zhang, Y., Yao, S., 2005. J. Biochem. Biophys. Methods 62, 191–205.
Hubert, C., Houot, A.M., Corvol, P., Soubrier, F., 1991. J. Biol. Chem. 266, 15377–15383.
Janshoff, A., Galla, H.J., Steinem, C., 2000. Angew. Chem. 39, 4004–4032.
Jiang, X., Cao, Z., Tang, H., Tan, L., Xie, Q., Yao, S., 2008. Electrochem. Commun. 10, 1235–1237.
Jimsheena, V.K., Gowda, L.R., 2009. Anal. Chem. 81, 9388–9394.
Johnson, T.O., Ermolieff, J., Jirousek, M.R., 2002. Nat. Rev. Drug Discov. 1, 696–709.
Kao, P., Patwardhan, A., Allara, D., Tadigadapa, S., 2008. Anal. Chem. 80, 5930–5936.
Kumar, R.S., Thekkumkara, T.J., Sen, G.C., 1991. J. Biol. Chem. 266, 3854–3862.
Lederera, T., Stehrerb, B.P., Bauerb, S., Jakobya, B., Hilbera, W., 2010. Procedia Eng. 5, 959–964.
Liu, M., Zhang, Y., Yang, Q., Xie, Q., Yao, S., 2006. J. Agric. Food Chem. 54, 4087–4094.
Mancini, G.B.J., Henry, G.C., Macaya, C., O'Neill, B.J., Pucillo, A.L., Carere, R.G., Wargovich, T.J., Mudra, H., Luscher, T.F., Klibaner, M.I., Haber, H.E., Uprichard, A.C.G., Pepine, C.J., Pitt, B., 1996. Circulation 94, 258–265.
Mao, Y., Wei, W., He, D., Nie, L., Yao, S., 2002. Anal. Biochem. 306, 23–30.
Martin, S.J., Granstaff, V.E., Frye, G.C., 1991. Anal. Chem. 63, 2272–2281.
Matsui, T., Matsufuji, H., Osajima, Y., 1992. Biosci. Biotechnol. Biochem. 56, 517–518.
Mayer, M., Meyer, B., 2000. J. Med. Chem. 43, 2093–2099.
Montserrat, A.S., Vicente, J.P., Ana, C.A., 2007. FEBS Lett. 581, 3449–3454.
Nishino, H., Murakawa, A., Mori, T., Okahata, Y., 2004. J. Am. Chem. Soc. 126, 14752–14757.
Noble, M.E.M., Endicott, J.A., Johnson, L.N., 2004. Science 303, 1800–1805.
Noel, M.A.M., Topart, P.A., 1994. Anal. Chem. 66, 484–491.
Ogi, H., Naga, H., Fukunishi, Y., Hirao, M., Nishiyama, M., 2009. Anal. Chem. 81, 8068–8073.
Okahata, Y., Kawase, M., Niikura, K., Ohtake, F., Furusawa, H., Ebara, Y., 1998. Anal. Chem. 70, 1288–1296.
Oliver von, A., Bömer, U., 2005. ChemBioChem 6, 481–490.
Peach, M.J., 1977. Physiol. Rev. 57, 313–370.
Prime, K., Whitesides, G., 1991. Science 252, 1164–1167.
Ryan, J.W., Ryan, U.S., Schultz, D.R., Whitaker, C., Chung, A., 1975. Biochem. J. 146, 497–499.
Sauerbrey, G.Z., 1959. Z. Phys. Chem. 155, 206–222.
Sentandreu, M.A., Toldra, F., 2006. Nat. Protocols 1, 2423–2427.
Skeggs, L.T., Marsh, W.H., Kahn, J.R., Shumway, N.P., 1954. J. Exp. Med. 99, 275–282.
Soubrier, F., AlhencGelas, F., Hubert, C., Allegrini, J., John, M., Tregear, G., Corvol, P., 1988. Proc. Natl. Acad. Sci. U. S. A. 85, 9386–9390.
Takahashi, S., Iida, M., Furusawa, H., Shimizu, Y., Ueda, T., Okahata, Y., 2009. J. Am. Chem. Soc. 131, 9326–9332.
Tang, Z., Kang, J., 2006. Anal. Chem. 78, 2514–2520.
Uzawa, H., Kamiya, S., Minoura, N., Dohi, H., Nishida, Y., Taguchi, K., Yokoyama, S., Mori, H., Shimizu, T., Kobayashi, K., 2002. Biomacromolecules 3, 411–414.
Wegner, G.J., Wark, A.W., Lee, H.J., Codner, E., Saeki, T., Fang, S., Corn, R.M., 2004. Anal. Chem. 76, 5677–5684.
Wei, L., Clauser, E., Alhenc Gelas, F., Corvol, P., 1992. J. Biol. Chem. 267, 13398–13405.
Williams, R.D., Upadhyayula, A.K., Bhethanabotla, V.R., 2007. Sens. Actuators B 122, 635–643.
Wu, J., Aluko, R.E., Muir, A.D., 2002. J. Chromatogr. A 950, 125–130.
Xie, Q., Wang, J., Zhou, A., Zhang, Y., Liu, H., Xu, Z., Yuan, Y., Deng, M., Yao, S., 1999a. Anal. Chem. 71, 4649–4656.
Xie, Q., Zhang, Y., Xu, M., Li, Z., Yuan, Y., Yao, S., 1999b. J. Electroanal. Chem. 478, 1–8.
Zhang, R., Xu, X., Chen, T., Li, L., Rao, P., 2000. Anal. Biochem. 280, 286–290.
Zhang, Y., Wang, M., Xie, Q., Wen, X., Yao, S., 2005. Sens. Actuators B 105, 454–463.